Ultrafast Band-Gap Shift Induced by a Strain Pulse in Semiconductor Heterostructures

A. V. Akimov,[1,2] A. V. Scherbakov,[2] D. R. Yakovlev,[1,2] C. T. Foxon,[3] and M. Bayer[1]

[1]*Experimentelle Physik II, University of Dortmund, D-44221 Dortmund, Germany*
[2]*A. F. Ioffe Physico-Technical Institute, 194021 St. Petersburg, Russia*
[3]*School of Physics and Astronomy, University of Nottingham, Nottingham NG7 2RD, United Kingdom*

(Received 3 April 2006; published 20 July 2006)

The conventional piezospectroscopic effect is extended to picosecond time scales by using ultrashort strain pulses injected into semiconductor heterostructures. The strain pulses with durations of ~10 ps are generated in a metal transducer film by intense femtosecond laser pulses. They propagate coherently in the GaAs/(Al, Ga)As heterostructure over a distance of 100 μm and shift the band gaps by several meV as detected optically for quantum well exciton resonances by pump-probe techniques and time-resolved photoluminescence.

DOI: 10.1103/PhysRevLett.97.037401 PACS numbers: 78.20.Hp, 63.20.Kr, 78.47.+p, 78.67.De

A fundamental of many topical concept proposals for new solid state functional units, in particular, those relying on coherence of the involved excitations, is the need for control of their energies on an ultrashort time scale. Sizable energy shifts of an electron resonance have been demonstrated by applying uniaxial stress (piezospectroscopic effect) for many years [1,2], but the challenging task is to realize them on picosecond time scales or faster. Recently developed methods of ultrafast acoustics allow generation and detection of coherent strain pulses in solids. The strain pulses with picosecond duration can be generated by hitting a metal film [3–5] or a semiconductor [6–9] with intense femtosecond laser pulses. The amplitude of such a strain pulse may reach values of $\sim 10^{-2}$. The heat pulse which follows the picosecond strain pulse has essentially a longer ($>10^{-7}$ s) duration and a long leading edge [10]. In conjunction with deformation potentials in typical semiconductors ~10 eV, the ultrafast strain-induced shift of an electronic resonance may be as large as 100 meV, which exceeds by 2 orders of magnitude shifts achieved in ac Stark experiments [11]. To the best of our knowledge, ultrafast strain pulses have never been used to address electronic states in nanostructures [12].

In this Letter, we demonstrate the effect of picosecond strain pulses on the energy of the exciton resonance in GaAs/(Al, Ga)As heterostructures. The dynamical band-gap shift on several meV observed in our experiments is a first step for realizing ultrafast control of electronic state energy in nanostructures.

The GaAs/$Al_{0.33}Ga_{0.67}As$ heterostructure for this study has been grown by molecular beam epitaxy on a (001) GaAs substrate. It consists of five GaAs single quantum wells (QWs) with widths 2.5, 5, 10, 20, and 30 nm (the widest QW is the closest to the substrate) separated by 20 nm wide $Al_{0.33}Ga_{0.67}As$ barriers. The total thickness of the structure varies from $l_0 = 94$ to 96 μm. A 100 nm Cr film, which plays the role of a picosecond thermoelastic transducer, was deposited on the back side [Fig. 1(a)]. For excitation, 0.3 ps pump pulses from a Ti:sapphire laser with a regenerative amplifier ($\lambda = 800$ nm, repetition rate 250 kHz, maximum energy per pulse 1 μJ) were used. The pump beam was sent through variable delay line 1 and focused (200 μm diameter spot) on the metal transducer [Fig. 1(b)]. The temperature range $T = 1.8$–200 K was used.

The strain pulses, being photogenerated in the metal film and transduced to the GaAs substrate, propagate through the substrate with the longitudinal sound velocity $s_{GaAs} = 4.8 \times 10^3$ m/s [Fig. 1(a)] and reach the heterostructure at a time $t_0 = l_0/s_{GaAs} \approx 20$ ns. The strain pulse effect on the electronic properties of the QWs was studied in the time domain by three different optical pump-probe techniques. First, we describe the experiments where the QW reflection

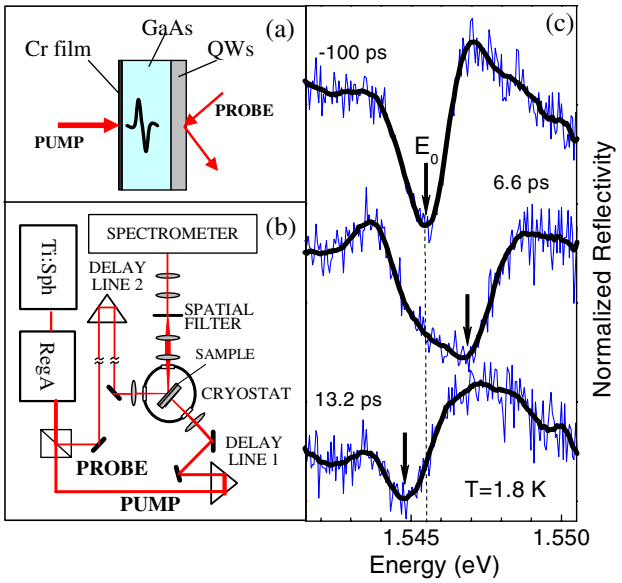

FIG. 1 (color online). (a) Sample, (b) experimental scheme, and (c) reflectivity spectra measured at different delay times $\Delta t = t - t_0$ ($t_0 \approx$ ns) for $W = 3$ mJ/cm^2. The vertical arrows in (c) indicate the energy of the exciton resonance. The solid lines show smoothed curves.

spectrum was recorded [Fig. 1(b)]. The probe beam (pulse energy ~1 pJ) was passed through delay line 2 to provide a fixed delay equal to t_0. It was focused to a spot with less than 50 μm diameter on the front side of the sample, precisely opposite to the pump spot. The probe beam reflected from the sample was collected by a fiber and guided to a spectrometer with a CCD camera. The spectral width of the probe pulses of 6.4 meV covers the heavy-hole exciton resonance at energy $E_0 \approx 1.546$ eV in the 10 nm GaAs QW for $T < 50$ K.

In the reflectivity spectrum, the QW exciton resonance is detected as a minimum. The upper curve in Fig. 1(c) shows the spectrum at a negative delay, $\Delta t = t - t_0 = -100$ ps, between the pump and probe when the strain pulse from the transducer did not yet arrive at the QW ($t = 0$ corresponds to the time when the pump pulse hits the metal film). It is identical with the reflectivity spectrum measured without a pump beam. With a pulse arrival at $t = t_0$, the spectrum changes. The main appearance is a shift of the resonance $\Delta E = E - E_0$. It moves first to higher energies up to $\Delta E \approx 1.5$ meV (see spectrum at $\Delta t = 6.6$ ps) and then to lower energies up to $\Delta E \approx -1.0$ meV ($\Delta t = 13.2$ ps) relative to the unperturbed spectrum.

To plot the time evolution of the exciton shift $\Delta E(t)$, the measured spectra were first smoothed [solid lines in Fig. 1(c)] and then the energy of the minimum indicated by the vertical arrows was evaluated. The results are given in Fig. 2(a) for a pump density $W = 3$ mJ/cm^2. The change of distance l_0 between excitation and detection points from 94 to 96 μm by choosing different points on the sample surface resulted in temporal shifts of $\Delta E(t)$ of about 420 ps. This agrees well with the time required for phonons to travel 2 μm in GaAs. This fact, together with the value of delay $t_0 = 20 \pm 0.2$ ns, confirms that the observed changes in reflection are caused by the strain pulse generated in the transducer.

The value of $\Delta E(t)$ is directly connected with the dynamical strain $\varepsilon_{QW}(t)$ in the QW:

$$\Delta E(t) = -[c - (a - b)]\varepsilon_{QW}(t), \tag{1}$$

where $a = -6$ eV, $b = -2$ eV ($c = 7.3$ eV) are the hole (electron) deformation potentials [13]. It is seen in Fig. 2(a) that $\Delta E(t)$ changes its sign several times during 100 ps. The high energy shift of the exciton resonance ($\Delta E > 0$) corresponds to compression and negative strain [$\varepsilon_{QW}(t) < 0$], while the low energy shift is caused by decompression [$\varepsilon_{QW}(t) > 0$]. The maximum shifts ΔE achieved in our experiments were 2 and -3 meV in the compression and decompression temporal parts, respectively.

We have analyzed the temporal $\Delta E(t)$ shape by an approach developed for ultrafast acoustics [3,4]. We model the temporal shape of the strain pulse injected into the GaAs substrate at the Cr/GaAs interface by a function which is a derivative of a Gaussian:

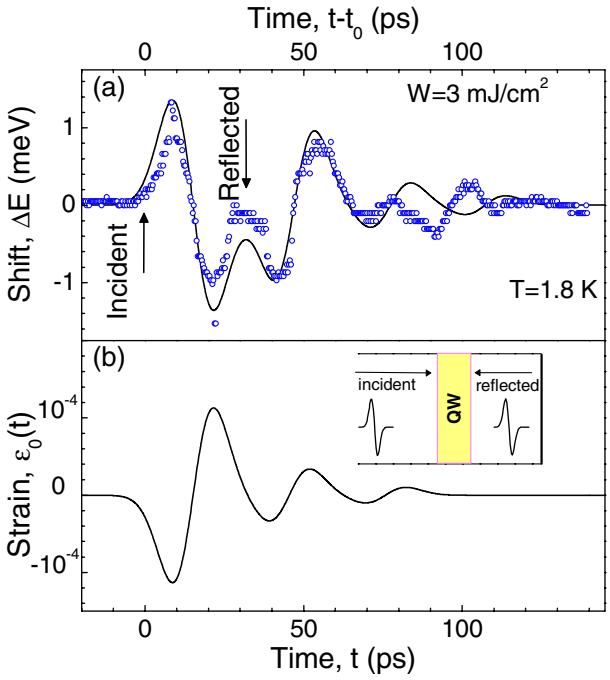

FIG. 2 (color online). (a) Measured (dots) and calculated (solid line) temporal evolution of the dynamical band-gap shift $\Delta E(t)$ induced by strain pulses in the 10 nm GaAs/$Al_{0.33}Ga_{0.67}As$ QW. The vertical arrows show the arrival of incident and expected reflected strain pulses. (b) Calculated temporal evolution of initial strain pulse $\varepsilon_0(t)$ injected from the metal transducer into the GaAs substrate. The inset shows schematically the incident and reflected strain pulses acting on the QW energy levels.

$$\varepsilon_0(t) = \frac{2A\xi}{s_{Cr}\tau^2}(1 - R)\sum_{j=0}^{\infty} R^j\left(t - \frac{(2j+1)d}{s_{Cr}}\right) \times \exp\left[-\frac{1}{\tau^2}\left(t - \frac{(2j+1)d}{s_{Cr}}\right)^2\right], \tag{2}$$

where $\xi = 12$ nm is the absorption length of the pump light ($\lambda = 800$ nm) in Cr, $R = 0.3$ is the reflection coefficient of longitudinal sound waves at the interface Cr/GaAs, $d = 100$ nm is the thickness of Cr film, and $s_{Cr} = 6.6 \times 10^3$ m/s is the longitudinal sound velocity in Cr. A is a dimensionless coefficient which depends on the pump density and transducer parameters [3]:

$$A = \frac{3(1 - r)W\beta B}{2C_{Cr}\xi\rho_{Cr}s_{Cr}^2}, \tag{3}$$

where $r = 0.7$ is the light reflection coefficient for Cr at $\lambda = 800$ nm, $\beta = 4.9 \times 10^{-6}$ 1/K is the linear expansion coefficient, $B = 160$ GPa is the bulk modulus, $C_{Cr} = 3.24 \times 10^6$ J/(m^3 K) is the specific heat, and $\rho_{Cr} = 7.2 \times 10^3$ kg/m^3 is the Cr density. In Eq. (2), $\tau \geq \xi/s_{Cr}$ is an adjustable parameter, which slightly increases the temporal width of $\varepsilon_0(t)$ relative to an ideal situation with $\tau = \xi/s_{Cr}$ The value of τ is governed by electron diffusion [3,4] and imperfections of the metal film. The summation in Eq. (2) accounts for multiple reflection of the photogenerated

strain pulse inside the transducer at the Cr/GaAs interface and the Cr surface. For each reflection cycle with a period of about 30 ps, a portion of strain is injected into the GaAs substrate.

Figure 2(b) shows the calculated temporal shape of $\varepsilon_0(t)$ for $W = 3$ mJ/cm^2 and $\tau = 8.3$ ps using Eqs. (2) and (3). It consists of sequential compression ($\varepsilon_0 < 0$) and decompression ($\varepsilon_0 > 0$). Assuming that this strain pulse propagates through the substrate and heterostructure and reaches the opposite surface without a change of shape in time (temporal transformation) and attenuation, we can model the temporal evolution of strain in the QW $\varepsilon_{\mathrm{QW}}(t)$ and calculate $\Delta E(t)$ using Eq. (1) [14]. We take into account that the strain pulse acts twice on the QW. The first time, the incident pulse hits the QW on its direct way from the transducer. The second time, the strain pulse hits the QW on the way back, after reflection at the free surface, where the strain pulse changes its phase [see inset in Fig. 2(b)]. The reflected strain pulse reaches the QW with a delay $t_r = 2l_r/\bar{s}$ relative to the first pulse. Here $\bar{s} \approx 5 \times 10^3$ m/s is the mean sound velocity in the (AlGa)As heterostructure; l_r is the distance from the QW to the free surface. In the studied structure, $l_r = 78.5$ nm for the 10 nm QW and, correspondingly, $t_r = 33$ ps. Thus, we may calculate $\varepsilon_{\mathrm{QW}}(t) = \varepsilon_0(t - t_0) - \varepsilon_0(t - t_0 - t_r)$. The resulting curve for $\Delta E(t)$ is shown by the solid line in Fig. 2(a) and is in good agreement with the measured time evolution.

Next, we present the results of pump-probe experiments where the probe beam was detected without spectrometer by a photodiode. We carried out: (a) conventional pump-probe experiments, where the intensity $R(t)$ of the reflected probe beam is measured as function of delay between pump and probe and (b) Kerr rotation experiments, where the polarization rotation angle $\theta(t)$ of the reflected light is detected [15]. The results obtained by these techniques are very similar. Figure 3(a) shows typical temporal signals for $\Delta R(t)/R$ and $\theta(t)$. The curves show oscillations with a period of 23 ps which are superimposed by several spikes in the Δt range from 0 up to 80 ps. The "oscillatory" part of the signal solely present for $\Delta t < 0$ and $\Delta t > 150$ ps is attributed to the elasto-optical effect, and the details of these oscillations and their application in ultrafast acoustics can be found in Refs. [7,8]. The "spike" part is due to pump-probe signals induced by the strain pulse arrival at the 10 nm QW. The behavior of $\Delta R(t)/R$ and $\theta(t)$ in the spike part is similar to the evolution of $\Delta E(t)$ in Fig. 2(a). This brings us to the conclusion that the spike part has the same origin as the dynamical exciton energy shift. The wavelength of the probe beam coincides with the exciton resonance transition only for the 10 nm QW, and therefore the contribution of this QW dominates in the detected signals. The inset in Fig. 3(a) shows the W dependence of the mean intensity of the reflectivity and Kerr signals in the spike part, which are calculated as $(\int_{t_1}^{t_2}[\Delta R(t)/R]^2 dt)^{1/2}$ and $(\int_{t_1}^{t_2}[\theta(t)]^2 dt)^{1/2}$, respectively. t_1 and t_2 are indicated by the vertical dashed lines in Fig. 3(a). We note that these dependencies are strongly sublinear, which highlights strong nonlinearities of the studied phenomenon.

Figure 3(b) shows the signals $\theta(t)$ for several lattice temperatures varied from 10 to 205 K. With increasing temperature, (i) the signal amplitude decreases in both the oscillatory and spike parts, and (ii) the starting point of the spike part shifts in time. We attribute these observations to the temperature dependencies of sound attenuation and sound velocity in GaAs. The attenuation is caused by interaction of high frequency components in the strain wave packet with thermal phonons. The Fourier transform of the modeled $\varepsilon_0(t)$ [Fig. 2(b)] gives a maximum at 30 GHz. From the decrease of $\theta(t)$ in Fig. 3(b) at higher T, we estimate the mean free path for the 30 GHz phonons to be equal to the sample thickness of $l_0 \approx 100$ μm at $T \approx 200$ K. The inset in Fig. 3(b) shows the relative change of sound velocity in GaAs as function of T, evaluated from the temporal shift of the spike shown by the arrows in the main panel. This dependence and also the mean free path estimate are in good agreement with previously published data [16]. The increase of T from 10 to 205 K obviously changes the position of the exciton resonances in 10 nm QW on a value 55 meV. This can lead to sensitivity and phase changes of the detected signal whose wavelength is fixed. Indeed, the changes of temporal evolution in the spike part are observed with the increase of T [Fig. 3(b)].

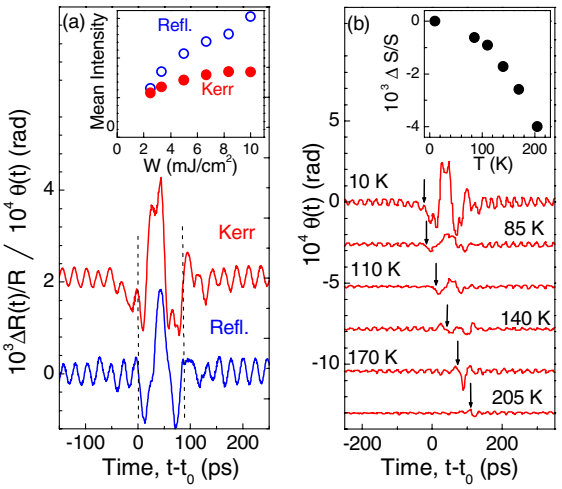

FIG. 3 (color online). Phonon-induced dynamics in a 10 nm GaAs/$Al_{0.33}Ga_{0.67}$As QW: (a) Reflectivity $\Delta R(t)/R$ and Kerr rotation $\theta(t)$ signals measured in pump-probe experiments without spectral resolution at $T = 10$ K and $W = 5$ mJ/cm^2. The inset shows the power dependence of the mean intensity for $\Delta R(t)/R$ (open symbols) and $\theta(t)$ (solid symbols) in the spike part of the signal (vertical dashed lines show the integration interval from 0 to 80 ps). (b) Kerr rotation signals measured at different temperatures for $W = 5$ mJ/cm^2. The vertical arrows indicate the arrival time of a strain pulse in a 10 nm QW. The inset shows the measured temperature dependence of sound velocity in GaAs.

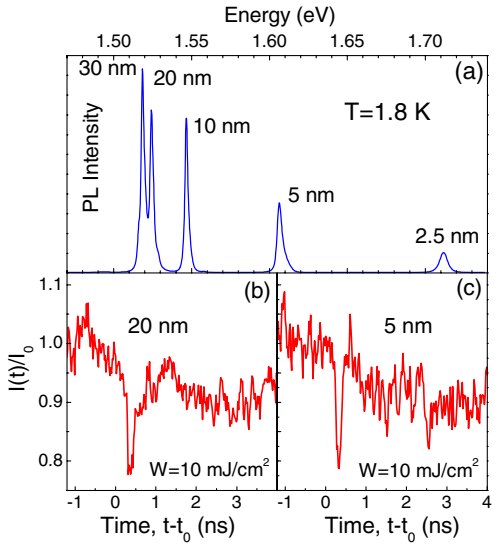

FIG. 4 (color online). (a) cw PL spectrum of the studied $GaAs/Al_{0.33}Ga_{0.67}As$ QW heterostructure. Temporal evolution of normalized peak PL intensity in (b) 20 and (c) 5 nm QWs induced by ultrafast strain pulses.

The detailed analysis of such behavior is out of the scope of the present work and will be reported elsewhere.

We turn now to the effect of strain pulses on the QW exciton photoluminescence (PL). The PL was excited by a pulsed laser (wavelength 630 nm, pulse duration 20 ns, pulse power 20 mW) synchronized with the pump laser. A cw PL spectrum measured at $T = 1.8$ K is shown in Fig. 4(a). It consists of spectral lines corresponding to recombination of heavy-hole exciton in the different QWs. In time-resolved experiments, the PL intensity $I(t)$ was detected by a streak camera attached to a spectrometer. Figures 4(b) and 4(c) show strain-induced PL signals $I(t)/I_0$, with I_0 being the intensity without pump for the 20 and 5 nm wide QWs. At $t = t_0 = 20$ ns, we see that $I(t)/I_0$ shows a sharp quenching of the PL emission in both QWs. The duration of these signals is limited by the time resolution 200 ps of our setup. We attribute this quenching to the band-gap shift induced by the strain pulse. One expects that strain may lead to a simultaneous decrease of $I(t)$ at one wavelength and an increase at another one. However, such redistribution is impossible to detect with 200 ps time resolution because the energy of the exciton resonance oscillates back and forth during times less than 100 ps [Fig. 2(a)]. This leads to a spectral smearing of the signal $I(t)/I_0$, and only the quenching of the central part of the exciton line is clearly observed.

It is important to mention that nonlinear effects in the strain pulse propagation lead to the formation of acoustic soliton train with a strain amplitude $\sim 10^{-2}$ [17–20]. Such a regime is perspective for obtaining band-gap shifts up to 100 meV. We already observe a nonlinear response to the pump density increase [inset in Fig. 3(a)], but to resolve the changes at high W, a more perfect metal transducer surface which provides a plane soliton front should be used [21].

To conclude, we have realized an ultrafast shift of the band-gap energy in GaAs/(Al, Ga)As semiconductor heterostructures by an action of picosecond strain pulses. The effect has been detected by several time-resolved techniques. A combination of the ultrafast acoustics with the piezospectroscopic effect opens a new direction in solid state physics, allowing the control of the electronic states energy on a picosecond time scale. This can form a new basis for realizing ultrafast manipulations in nanophotonic (e.g. photonic crystals) and nanoelectronic (e.g. tunneling diodes) devices.

We are thankful to D. Schemionek for sample preparation and to J. I. Dijkhuis, O. B. Wright, and A. A. Kaplyanskii for discussions. We acknowledge financial support of the BMBF (nanoquit), the DFG (research group on quantum optics), the RFBR, and the Russian Academy of Sciences. The Deutsche Forschungsgemeinschaft financed research stays of A. V. A. and A. V. S. (Grant No. 436 RUS 17/145/05) in Dortmund.

[1] E. F. Gross and A. A. Kaplyanskii, Sov. Phys. Solid State **2**, 1518 (1961).
[2] M. Cardona, *Modulation Spectroscopy* (Academic, New York, 1969).
[3] G. Tas and H. J. Maris, Phys. Rev. B **49**, 15 046 (1994).
[4] T. Saito, O. Matsuda, and O. B. Wright, Phys. Rev. B **67**, 205421 (2003).
[5] B. C. Daly, T. B. Norris, J. Chen, and J. B. Khurgin, Phys. Rev. B **70**, 214307 (2004).
[6] J. J. Baumberg, D. A. Williams, and K. Köhler, Phys. Rev. Lett. **78**, 3358 (1997).
[7] O. B. Wright, B. Perrin, O. Matsuda, and V. E. Gusev, Phys. Rev. B **64**, 081202(R) (2001).
[8] O. Matsuda, T. Tachizaki, T. Fukui, J. J. Baumberg, and O. B. Wright, Phys. Rev. B **71**, 115330 (2005).
[9] S. H. Lee *et al.*, Phys. Rev. Lett. **95**, 246104 (2005).
[10] R. J. von Gutfeld, in *Physical Acoustics*, edited by W. P. Mason (Academic, New York, 1958), Vol. 5, p. 233.
[11] M. Saba *et al.*, Phys. Rev. B **62**, R16 322 (2000).
[12] For microsecond experiments, see T. Kobayashi, T. Sekine, Xijun Li, and Y. Yamashita, Phys. Rev. B **69**, 054108 (2004), and references therein.
[13] F. H. Pollak and M. Cardona, Phys. Rev. **172**, 816 (1968).
[14] We neglect the finite width of QWs and consider a QW as a delta layer.
[15] *Semiconductor Spintronics and Quantum Computation*, edited by D. D. Awschalom, D. Loss, and N. Samarth (Springer-Verlag, Berlin, 2002).
[16] W. Chen *et al.*, Philos. Mag. B **70**, 687 (1994).
[17] H.-Y. Hao and H. J. Maris, Phys. Rev. B **64**, 064302 (2001).
[18] E. Pěronne and B. Perrin, Ultrasonics (to be published).
[19] O. L. Muskens and J. I. Dijkhuis, Phys. Rev. Lett. **89**, 285504 (2002).
[20] O. L. Muskens, A. V. Akimov, and J. I. Dijkhuis, Phys. Rev. Lett. **92**, 035503 (2004).
[21] H.-Y. Hao and H. J. Maris, Phys. Rev. B **63**, 224301 (2001).